

# Structure of a complex of *Thermoactinomyces vulgaris* R-47 $\alpha$ -amylase 2 with maltohexaose demonstrates the important role of aromatic residues at the reducing end of the substrate binding cleft

Akashi Ohtaki,<sup>a</sup> Masahiro Mizuno,<sup>b</sup> Hiromi Yoshida,<sup>c</sup> Takashi Tonozuka,<sup>b</sup>  
Yoshiyuki Sakano<sup>b</sup> and Shigehiro Kamitori<sup>a,c,\*</sup>

<sup>a</sup>Department of Biotechnology and Life Science, Tokyo University of Agriculture and Technology, 2-24-16 Naka-cho, Koganei, Tokyo 184-8588, Japan

<sup>b</sup>Department of Applied Biological Science, Tokyo University of Agriculture and Technology, 3-5-8 Saiwai-cho, Fuchu, Tokyo 183-8509, Japan

<sup>c</sup>Molecular Structure Research Group, Information Technology Center, Kagawa University, 1750-1 Ikenobe, Miki-cho, Kita-gun, Kagawa 761-0793, Japan

Received 15 September 2005; received in revised form 6 January 2006; accepted 10 January 2006

Available online 27 March 2006

**Abstract**—*Thermoactinomyces vulgaris* R-47  $\alpha$ -amylase 2 (TVAII) can efficiently hydrolyze both starch and cyclomaltooligosaccharides (cyclodextrins). The crystal structure of an inactive mutant TVAII in a complex with maltohexaose was determined at a resolution of 2.1 Å. TVAII adopts a dimeric structure to form two catalytic sites, where substrates are found to bind. At the catalytic site, there are many hydrogen bonds between the enzyme and substrate at the non-reducing end from the hydrolyzing site, but few hydrogen bonds at the reducing end, where two aromatic residues, Trp356 and Tyr45, make effective interactions with a substrate. Trp356 drastically changes its side-chain conformation to achieve a strong stacking interaction with the substrate, and Tyr45 from another molecule forms a water-mediated hydrogen bond with the substrate. Kinetic analysis of the wild-type and mutant enzymes in which Trp356 and/or Tyr45 were replaced with Ala suggested that Trp356 and Tyr45 are essential to the catalytic reaction of the enzyme, and that the formation of a dimeric structure is indispensable for TVAII to hydrolyze both starch and cyclodextrins. © 2006 Elsevier Ltd. All rights reserved.

**Keywords:** X-ray structure;  $\alpha$ -Amylase; Maltohexaose; Enzymatic glucoside hydrolysis

## 1. Introduction

$\alpha$ -Amylase [ $\alpha$ -(1→4)-D-glucan-4-glucanohydrolase; EC 3.2.1.1] belonging to glycoside hydrolase family 13,<sup>1</sup> catalyzes the hydrolysis of  $\alpha$ -(1→4)-D-glucosidic linkages in starch to liberate products: maltooligosaccharides, with net retention of anomeric configuration. Generally,  $\alpha$ -amylase has three strictly conserved catalytic residues, two Asp and a Glu, and three typical domains; domain A with a ( $\beta/\alpha$ )<sub>8</sub> barrel, domain B being a loop protruding from domain A, and domain C with a  $\beta$ -sandwich structure.<sup>2</sup> The structures of domains A and C are well conserved, while the structure of domain B has been found to vary.

**Abbreviations:** TVAI, *Thermoactinomyces vulgaris* R-47  $\alpha$ -amylase 1; TVAII, *Thermoactinomyces vulgaris* R-47  $\alpha$ -amylase 2; CD, cyclodextrin; D325N, inactive mutant TVAII (Asp325→Asn); G6, maltohexaose; D325N/G6, inactive mutant TVAII complex with maltohexaose; Y45A, mutant TVAII (Tyr45→Ala); W356A, mutant TVAII (Trp356→Ala); TAA, *Aspergillus oryzae*  $\alpha$ -amylase; BA2, *Bacillus licheniformis*  $\alpha$ -amylase; MES, 4-morpholineethanesulfonic acid.

\*Corresponding author at present address: Molecular Structure Research Group, Information Technology Center, Kagawa University, 1750-1 Ikenobe, Miki-cho, Kita-gun, Kagawa 761-0793, Japan. Tel./fax: +81 87 891 2421; e-mail: [kamitori@med.kagawa-u.ac.jp](mailto:kamitori@med.kagawa-u.ac.jp)

*Thermoactinomyces vulgaris* R-47 produces two  $\alpha$ -amylases, TVAI (637 amino acids, MW = 71,000 Da), and TVAII (585 amino acids, 67,500 Da).<sup>3</sup> In addition to hydrolyzing starch, these two enzymes have unusual activities for cyclomaltooligosaccharides (cyclodextrins, CD), which are little hydrolyzed by other  $\alpha$ -amylases.<sup>3</sup> TVAII as an intracellular enzyme can efficiently hydrolyze  $\alpha$ -,  $\beta$ -, and  $\gamma$ -CDs (six, seven, and eight glucose units), by what is called cyclodextrinase activity.<sup>4</sup> To elucidate the properties of TVAs, we reported the X-ray structures of TVAI,<sup>5</sup> TVAII,<sup>6</sup> and an inactive mutant TVAII in a complex with CDs,<sup>7,8</sup> and conducted the kinetic analyses of mutant TVAIIs,<sup>9</sup> obtaining new insight into the mechanism behind the recognition of CDs.

TVAII has an extra domain N with a distorted  $\beta$ -barrel structure, in addition to the three common domains, and forms a dimeric structure using domain N as a connector, to give suitable catalytic site clefts for CDs. The X-ray structures of three enzymes having hydrolyzing activity for CDs, maltogenic  $\alpha$ -amylase (ThMA),<sup>10</sup> *Bacillus stearothermophilus* neopullulanase,<sup>11</sup> and cyclomaltodextrinase,<sup>12</sup> have been reported, showing that they too form a dimeric structure using domain N. Therefore, the formation of a dimeric structure is thought to be indispensable for the recognition of CDs. However, it is not clear whether a dimeric structure of TVAII is required for the hydrolyzing of starch, and/or how TVAII recognizes starch as a substrate in a dimeric structure, because almost all  $\alpha$ -amylases function as a monomer structure. We therefore examined the X-ray structure of an inactive mutant TVAII (D325N, Asp325→Asn) in a complex with maltohexaose (G6) at a resolution of 2.1 Å, finding that two aromatic residues (Tyr45 and Trp356) interacting with a

substrate at the reducing end side were needed to recognize substrates. To confirm this, we also carried out kinetic analyses of TVA II hydrolyzing activities for starch and  $\beta$ -CD, using the wild-type TVA II and two mutant enzymes, Y45A and W356A.

## 2. Results and discussion

### 2.1. Overall structure of D325N/G6

Figure 1<sup>13,14</sup> shows the overall structure of the D325N/G6 complex. TVAII is composed of four domains; domain N (residue 1–121) with a distorted  $\beta$ -barrel structure, domain A (122–242 and 298–502) with a  $(\beta/\alpha)_8$  barrel structure, domain B (243–297) protruding from domain A, and domain C (503–585) with a  $\beta$ -sandwich structure. TVAII forms a dimeric structure of two molecules, denoted Mol-1 and Mol-2, related by non-crystallographic 2-fold symmetry. In the dimeric structure, there are two catalytic sites that are formed by the residues from domains A and B, and partially by domain N of another molecule. Since in structure Mol-1 and Mol-2 are almost identical, with the r.m.s. deviations between them being 0.860 Å for main-chain atoms, and the substrate binding mode is almost identical between Mol-1 and Mol-2. Here, the structural description concentrates on the catalytic site located in Mol-1, and residues from Mol-2 are indicated by '\*' for clarity, for example, Tyr45\*.

### 2.2. Catalytic site structure with maltohexaose (G6)

The omit map for the binding of G6 in Mol-1 with a  $4.0\sigma$  contoured level is illustrated in Figure 2.<sup>15</sup> Glucose

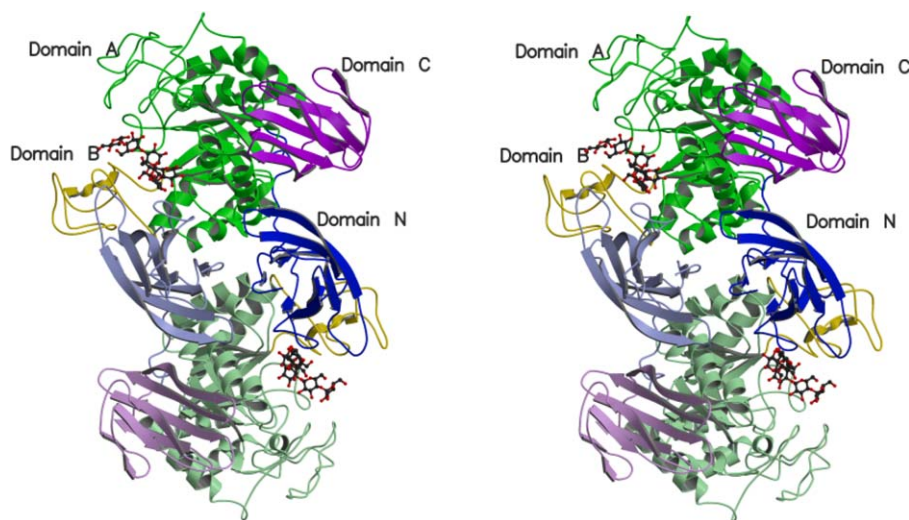


**Figure 1.** Stereoview of overall structure of the D325N/G6 complex illustrated by the program MOLSCRIPT.<sup>13</sup> Domain N, A, B, and C are colored in blue, green, yellow, and magenta, respectively. Mol-2 is shown by light colors. G6s are represented by a wire model.

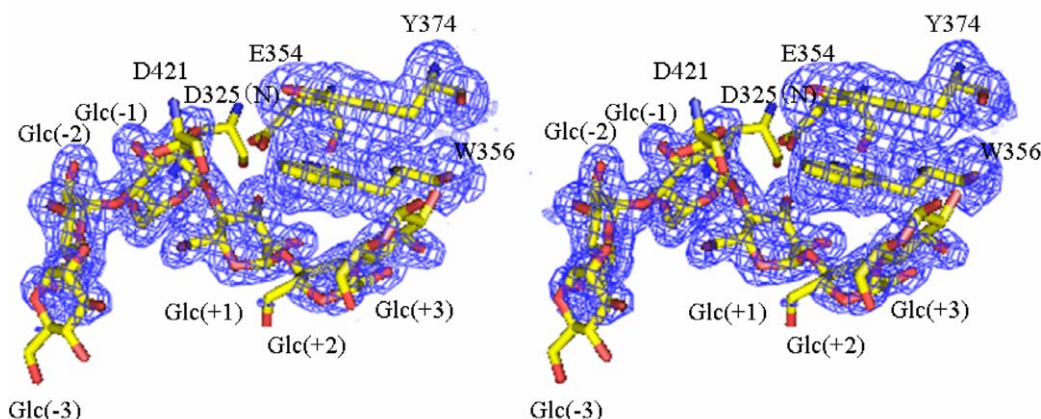


**Figure 2.** Stereoview of the simulated annealed omit maps with a structural model of bound G6. The contoured level of this map is  $4.0\sigma$ , illustrated by the program PYMOL.<sup>15</sup>

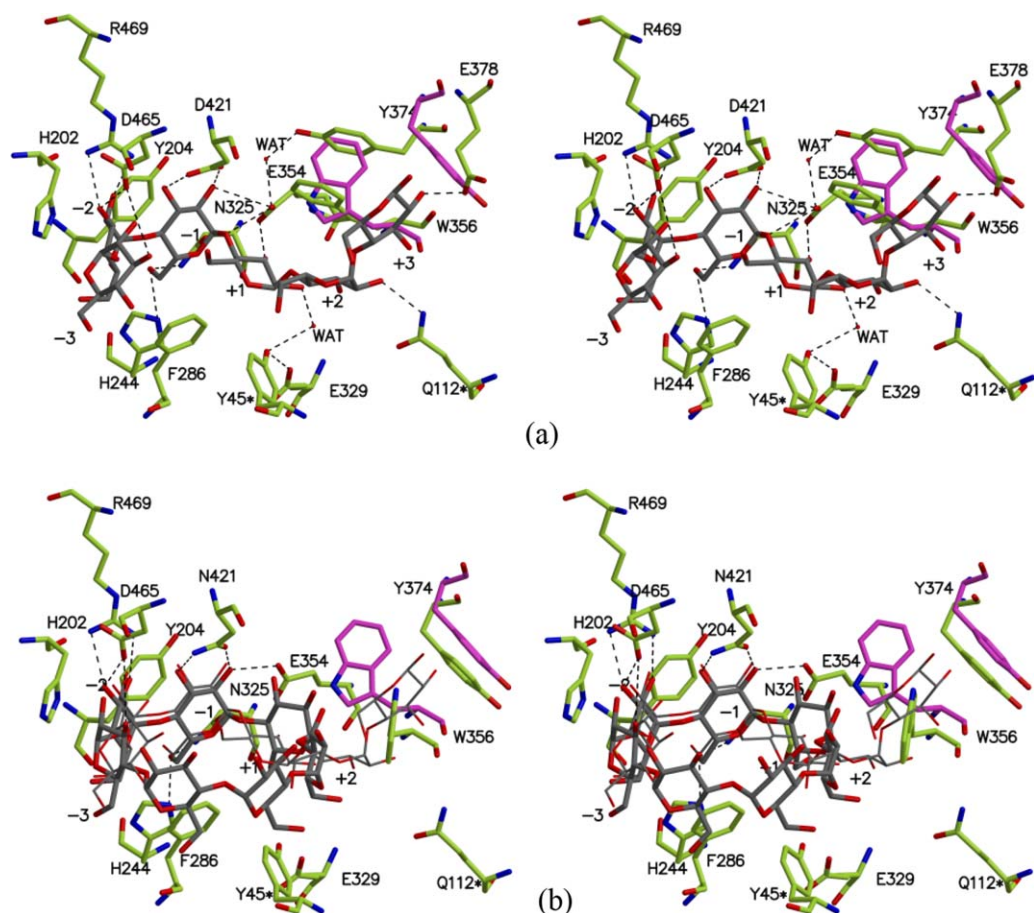
units of G6 are designated Glc(−3), Glc(−2), Glc(−1), Glc(+1), Glc(+2), and Glc(+3) from the non-reducing to reducing end. The numbers in parentheses indicate the subsites, and the hydrolyzing site is between subsites −1 and +1. The glucosidic bond between Glc(−1) and Glc(+1) is intact, and the conformation of the pyranoside in the subsite −1 is a  ${}^4C_1$  chair form. The quality of the electron density maps of Glc(−3) and Glc(+3) is not good enough to locate all the atoms in glucose units, suggesting that Glc(−3) and Glc(+3) are highly disordered.

Figure 3 shows the interaction between the enzyme and G6. The torsion angles of the glycosidic bonds of G6 at the hydrolyzing site,  $\varphi = 41^\circ$  (O-5–C-1–O-4'–C-4') and  $\psi = -149^\circ$  (C-1–O-4'–C-4'–C-5') deviate greatly from those of the regular helical structure of amylose;  $\varphi = 104^\circ$  and  $\psi = -121^\circ$ .<sup>16</sup> The three catalytic residues that are strictly conserved in  $\alpha$ -amylases are in TVAII, Asn325, Glu354, and Asp421. According to the proposed hydrolyzing mechanism, the O-E atom of Glu354 protonates the O-4 atom (glycosidic oxygen) at a hydrolyzing site, which is followed by the attack of the O-D atom of Asp325 on the C-1 atom of Glc(−1), and Asp421 is involved in fixing the substrate and in stabilizing the transition state.<sup>17,18</sup> In D325N/G6, the O-E1 atom of Glu354 forms a hydrogen bond with the glycoside oxygen atom (O-4 atom) between Glc(−1) and Glc(+1), and the ND1 atom of Asn325 forms a hydrogen bond with the O-6 atom of Glc(−1), causing the O-D1 atom to be in direct contact with the C-1 atom of Glc(−1) with a distance of 3.0 Å. The O-D1 and O-D2 atoms of Asp421 form hydrogen bonds with the O-2 and O-3 atoms of Glc(−1) to fix its orientation. Thus, the interactions of the three catalytic residues of TVAII with G6 well support the proposed catalytic mechanism of  $\alpha$ -amylase. In addition, there are many interactions between the enzyme and G6 at (−) subsites. Asp465 forms hydrogen bonds with the O-3 atom of

Glc(−2) and O-2 atom of Glc(−3), and Arg469 also makes hydrogen bonds with the O-2 and O-3 atoms of Glc(−2). Two planar residues form nicely stacking interactions with G6; they are Tyr204 with Glc(−1) and His202 with Glc(−2).

By contrast, few direct hydrogen bonds exist between the enzyme and G6 at (+) subsites, only Gln112\*–Glc(+2) and Glu378–Glc(+3), compared to the number in other  $\alpha$ -amylase/oligosaccharide complexes.<sup>19,20</sup> Instead of direct hydrogen bonds, Trp356 and Tyr45\* make favorable interactions with Glc(+1) and Glc(+2) of G6, helping to fix the substrate in a proper position. Through the binding of G6, Trp356 and Tyr374 change their side-chain conformations to make strong stacking interactions with Glc(+2). Trp356 and Tyr374 in unliganded TVAII are superimposed in Figure 3a. Due to the stacking interactions of Trp356 with Glc(+2), G6 is bent at the hydrolyzing site, directing the O-4 atom (glycoside oxygen) to Glu354 to form a hydrogen bond. Thus, Trp356 plays an important role in stabilizing the conformation of G6 for the catalytic reaction. Figure 3b shows the previously reported TVAII/ $\beta$ -CD structure, where Trp356 interacted with  $\beta$ -CD in a different manner from G6. These enzyme–substrate complex structures showed that Trp356 certainly interacts with a glucose unit at subsite +2; therefore, Trp356 is thought to be responsible for the multiple substrate-recognition mechanism of TVAII, by changing its side-chain conformation depending on the substrate to stabilize enzyme–substrate complex. Tyr45\* forms an intermolecular (Mol-1 and Mol-2) hydrogen bond with Glu329 to construct part of the active cleft, and makes a water-mediated hydrogen bond with the O-2 atom of Glc(+1) and van der Waals contacts with Glc(+1) and Glc(+2). Since the Tyr45 residue of domain N is conserved in neopullulanase<sup>11</sup> and maltogenic  $\alpha$ -amylase<sup>10</sup> with hydrolyzing activity for CDs, Tyr45 is proposed to be essential for recognizing CDs. This study showed that Tyr45 may also play an





**Figure 3.** Stereoviews of interactions between catalytic site residues (yellow) and G6 (gray) (a), and  $\beta$ -CD (gray) (b), illustrated by the program MOLSCRIPT.<sup>13</sup> Trp356 and Tyr374 in the unliganded TVAII are superimposed (magenta), and G6 is superimposed with thin lines in (b). The selected hydrogen bonds are shown with dotted lines.

important role in the enzyme–substrate interactions at (+) subsites in the hydrolysis of starch.

### 2.3. Kinetic analyses of W356A and Y45A

Strong interactions at the reducing end between G6 and two aromatic residues, Tyr45\* and Trp356, were observed through the binding of G6. To confirm the role

of Tyr45\* and Trp356, we constructed mutant TVAII, W356A (Trp356→Ala), and Y45A (Tyr45→Ala), by site-directed mutagenesis, and carried out a kinetic analysis for starch and  $\beta$ -CD. The kinetic parameters of the wild-type TVA II, W356A, and Y45A are listed in Table 1. All mutant enzymes exhibited a reduction in activity for both substrates to 1.0–5.0% of the  $k_{\text{cat}}/K_{\text{m}}$  values compared to wild-type TVAII, showing that

**Table 1.** Kinetic parameters of wild-type TVAII and mutant enzymes

	W356A	Y45A	Wild-type
$K_{\text{m}}$ (mM)			
$\beta$ -CD	$1.94 \pm 0.10(146)$	$2.82 \pm 0.33(215)$	$1.31 \pm 0.08(100)^{\text{b}}$
Starch	$0.95 \pm 0.06^{\text{a}}(317)$	$2.60 \pm 0.45^{\text{a}}(867)$	$0.30 \pm 0.01^{\text{a}}(100)^{\text{b}}$
$k_{\text{cat}}$ ( $\text{s}^{-1}$ )			
$\beta$ -CD	$1.06 \pm 0.29(2.4)$	$2.08 \pm 0.54(4.8)$	$43.40 \pm 1.30(100)^{\text{b}}$
Starch	$0.72 \pm 0.21(2.5)$	$12.56 \pm 3.00(44.0)$	$28.52 \pm 0.32(100)^{\text{b}}$
$k_{\text{cat}}/K_{\text{m}}$ ( $\text{s}^{-1} \text{mM}^{-1}$ )			
$\beta$ -CD	$0.55 \pm 0.17(1.7)$	$0.74 \pm 0.24(2.2)$	$33.13 \pm 0.92(100)^{\text{b}}$
Starch	$0.90 \pm 0.38(1.0)$	$4.79 \pm 0.50(5.0)$	$94.32 \pm 3.40(100)^{\text{b}}$

<sup>a</sup>  $K_{\text{m}}$  values of starch were % (w/v).

<sup>b</sup> The ratio of each kinetic parameter for each mutant relative to the wild-type enzyme (%) is given in parentheses.

Trp356 and Tyr45\* are required for the activity of TVAII to hydrolyze starch and CDs.

The  $K_m$  values of W356A for  $\beta$ -CD and starch are 146% and 317% that of wild-type TVAII, respectively. The  $k_{cat}$  value of W356A for both substrates is more decreased compared to wild-type TVAII and Y45A. These results showed that the Trp356 residue plays an important role for catalytic reaction, and the replacement of Trp356 by Ala is expected to affect the stability of the enzyme–substrate complex, especially the transition state, in which the binding of starch is much more than in the binding of  $\beta$ -CD.

In Y45A, this tendency is more remarkable. The  $K_m$  values of Y45A for  $\beta$ -CD and starch are 215 and 867% that of wild-type TVAII, respectively. While, the  $k_{cat}$  value of Y45A for starch is not decreased as well as for  $\beta$ -CD. These results showed that Tyr45 plays an important role for substrate binding.

In other  $\alpha$ -amylase–ligand complexes,<sup>21–24</sup> *Aspergillus oryzae*  $\alpha$ -amylase (TAA) with acarbose,<sup>21</sup> *Bacillus licheniformis*  $\alpha$ -amylase (BA2) with acarbose,<sup>22</sup> the aromatic residues (Tyr155; TAA, Tyr193; BA2) from domain B are located at the reducing end, and strongly interact with Glc(+2). This aromatic residue is conserved in these amylases. TVAII has no residues from Mol-1 at the reducing end corresponding to these aromatic residues, because the loop region of domain B is shorter than in other  $\alpha$ -amylases. In TVAII, the residues from the loop region (42\*–50\*) of Mol-2 construct part of the catalytic site by forming a dimeric structure, and Tyr45\* is thought to play a role in place of these aromatic residues as found in other  $\alpha$ -amylases. Therefore, the interaction of Tyr45\* with the substrate is essential to the catalytic reaction of TVAII, and the formation of a dimeric structure is indispensable for TVAII to hydrolyze starch as well as CDs.

### 3. Experimental

#### 3.1. Materials

All of the mutant enzymes were prepared from recombinant *Escherichia coli* MV1184 cells. Oligonucleotide-directed mutagenesis was carried out using the plasmid pTNKK with a Quick Change kit (Stratagene) for the construction of mutant enzymes D325N, W356A, and Y45A.

#### 3.2. X-ray crystallography

These mutant enzymes were purified in the same way as the wild-type TVAII.<sup>6</sup> Crystals of D325N were prepared by a vapor diffusion hanging drop method at 20 °C, using a protein (15 mg/mL) and a reservoir solution containing 1.0% (w/v) polyethylene glycol 6000 and

**Table 2.** Data collection and refinement statistics

D325N/maltohexaose complex	
Temperature (K)	100
Resolution (Å)	2.1
No. of measured refs.	469,220
No. of unique refs.	85,196
Completeness (%)	95.5 (97.2)
$R_{merge}$ <sup>a</sup>	0.078 (0.220) <sup>b</sup>
$I_0/\sigma(I_0)$	12.5 (4.5) <sup>b</sup>
Space group	$P2_12_12_1$
Cell dimensions	
$a$ (Å)	113.69
$b$ (Å)	118.71
$c$ (Å)	112.38
Structure refinement	
Resolution range (Å)	46.37–2.1
No. of refs.	85,196
Completeness (%)	95.5 (97.2) <sup>b</sup>
$R$	0.184 (0.225) <sup>b</sup>
$R_{free}$	0.231 (0.304) <sup>b</sup>
r.m.s.d. bond lengths (Å)	0.006
r.m.s.d. bond angles (°)	1.3

<sup>a</sup>  $R_{merge} = \sum \sum |I_i - \langle I \rangle| / \sum \langle I \rangle$ .

<sup>b</sup> The values for the highest resolution shell are given in parentheses (2.10–2.37 Å resolution).

2.5 mM calcium chloride in 20 mM MES buffer (pH 6.1). Crystals of D325N/G6 were obtained by a soaking method using the reservoir solution containing 1 mM G6 for 2 h.

X-ray diffraction data for D325N/G6 were collected at 100 K using an MacScience/DIP2040 imaging plate detector system on the BL44XU beam line in SPring-8 (Hyogo, Japan), with a cryoprotected solution containing 20% (w/v) of 2-methyl-2,4-pentadiol. Diffraction data were processed using HKL2000.<sup>25</sup> The collected data and scaling results are listed in Table 2. The initial phase was determined with a molecular replacement method using the structure of wild-type TVAII as a probe with the program CNS.<sup>26</sup> Models were corrected on the 2Fo-Fc electron density map using the program xFIT in the Xtalview system,<sup>27</sup> and structures without solvent molecules were refined using maximum resolution data. Solvent molecules were gradually introduced if peaks above  $4.0\sigma$  in the Fo-Fc electron density map were in the range of a hydrogen bond. To avoid the overfitting of diffraction data, a free  $R$ -factor with 10% of the test set excluded from refinement was monitored. Refinement of the final structure was converged at an  $R$ -factor of 0.184 ( $R_{free} = 0.217$ ) and refinement statistics are listed in Table 2. In a Ramachandran plot, 86.7% of residues are shown in the most favored regions as determined by the program PROCHECK,<sup>28,29</sup> and no residue is in disallowed regions.

#### 3.3. Enzyme assays

The activities for starch and  $\beta$ -CD were assayed as described.<sup>5</sup> The enzyme reaction was carried out in

100 mM phosphate buffer (pH 6.0) at 40 °C. The products were analyzed by the Nelson–Somogyi method for starch and  $\beta$ -CD by monitoring the reducing power of the hydrolysate. Wild-type TVaII and both mutant enzymes are confirmed to form a dimeric structure under the condition of the activity assay by a gel-filtration chromatography.

#### 4. Supplementary data

The coordinates and structural factors of the D325N/G6 complex were deposited in the Protein Data Bank under the accession codes 2D2O.

#### Acknowledgments

This study was supported by a Grant-in-Aid for Scientific Research (16370048) from the Ministry of Education, Culture, Sports, Science and Technology of Japan. This research was performed with the approval of SPring-8, Institute for Protein Research (Proposal C02A44XU-7111-N for BL44XU).

#### References

- Coutinho, P. M.; Henrissat, B. Carbohydrate-Active Enzymes server at URL: <http://afmb.cnrs-mrs.fr/CAZY/>, 1999.
- Berman, H. M.; Westbrook, J.; Feng, Z.; Gilliland, G.; Bhat, T. N.; Weissig, H.; Shendyalov, I. N.; Bourne, P. E. *Nucleic Acids Res.* **2000**, *28*, 235–242.
- Tonozuka, T.; Mogi, S.; Shimura, Y.; Ibuka, A.; Sakai, H.; Matsuzawa, H.; Sakano, Y.; Ohta, T. *Biochim. Biophys. Acta* **1995**, *1252*, 35–42.
- Park, K.-H.; Kim, T.-J.; Cheong, T.-K.; Kim, J.-W.; Oh, B.-H.; Svensson, B. *Biochim. Biophys. Acta* **2000**, *1478*, 165–185.
- Kamitori, S.; Abe, A.; Ohtaki, A.; Kaji, A.; Tonozuka, T.; Sakano, Y. *J. Mol. Biol.* **2002**, *318*, 443–453.
- Kamitori, S.; Kondo, S.; Okuyama, K.; Yokota, T.; Shimura, Y.; Tonozuka, T.; Sakano, Y. *J. Mol. Biol.* **1999**, *287*, 907–921.
- Kondo, S.; Ohtaki, A.; Tonozuka, T.; Sakano, Y.; Kamitori, S. *J. Biochem.* **2001**, *129*, 423–428.
- Ohtaki, A.; Mizuno, M.; Tonozuka, T.; Sakano, Y.; Kamitori, S. *J. Biol. Chem.* **2004**, *279*, 31033–31040.
- Ohtaki, A.; Kondo, S.; Shimura, Y.; Tonozuka, T.; Sakano, Y.; Kamitori, S. *Carbohydr. Res.* **2001**, *334*, 309–313.
- Kim, J.-S.; Cha, S.-S.; Kim, H.-J.; Kim, T.-J.; Ha, N.-C.; Oh, S.-T.; Cho, H.-S.; Cho, M.-J.; Kim, M.-J.; Lee, H.-S.; Kim, J.-W.; Choi, K.-Y.; Park, K.-H.; Oh, B.-H. *J. Biol. Chem.* **1999**, *274*, 26279–26286.
- Hondoh, H.; Kuriki, T.; Matsuura, Y. *J. Mol. Biol.* **2003**, *326*, 177–188.
- Fritzsche, H. B.; Schwede, T.; Schulz, G. E. *Eur. J. Biochem.* **2003**, *270*, 2332–2341.
- Kraulis, P. J. *J. Appl. Crystallogr.* **1991**, *24*, 946–950.
- Merritt, E. A.; Bacon, D. J. *Methods Enzymol.* **1997**, *277*, 505–524.
- Delano, W. L. *The PYMOL Molecular Graphic System*; DeLano Scientific: California, 2002.
- Imberty, A.; Chanzy, H.; Perez, S.; Buleon, A.; Tran, V. *J. Mol. Biol.* **1988**, *201*, 365–378.
- Sinnott, M. L. *Chem. Rev.* **1990**, *90*, 1171–1202.
- McCarter, J. D.; Withers, S. G. *Curr. Opin. Struct. Biol.* **1994**, *4*, 885–892.
- Fujimoto, Z.; Takase, K.; Doui, N.; Momma, M.; Matsumoto, T.; Mizuno, H. *J. Mol. Biol.* **1998**, *277*, 393–407.
- Robert, X.; Haser, R.; Mori, H.; Svensson, B.; Aghajari, N. *J. Biol. Chem.* **2005**, *280*, 32968–32978.
- Brzozowski, A. M.; Davies, G. J. *Biochemistry* **1997**, *36*, 10837–10845.
- Brzozowski, A. M.; Lawson, D. M.; Turkenburg, J. P.; Bisgaard-Frantzen, H.; Svendsen, A.; Borchert, T. V.; Dauter, Z.; Wilson, K. S.; Davies, G. J. *Biochemistry* **2000**, *39*, 9099–9107.
- Qian, M.; Nahoum, V.; Bonicel, J.; Bischoff, H.; Henrissat, B.; Payan, F. *Biochemistry* **2001**, *40*, 7700–7709.
- Davies, G. J.; Brzozowski, A. M.; Dauter, Z.; Rasmussen, M. D.; Borchert, T. V.; Wilson, K. S. *Acta Crystallogr.* **2005**, *D61*, 190–193.
- Otwinowski, Z.; Minor, W. *Methods Enzymol.* **1997**, *276*, 307–326.
- Brünger, A. T.; Adams, P. D.; Clore, G. M.; DeLano, W. L.; Gros, P.; Grosse-Kunstleve, R. W.; Jiang, J. S.; Kuszewski, J.; Nilges, M.; Pannu, N. S.; Read, R. J.; Rice, L. M.; Simonson, T.; Warren, G. L. *Acta Crystallogr. Sect. D* **1998**, *54*, 905–921.
- McRee, D. E. *J. Struct. Biol.* **1999**, *125*, 156–165.
- Ramachandran, G. N.; Sasisekharan, V. *Adv. Protein Chem.* **1968**, *23*, 283–437.
- Laskowski, R. A.; MacArthur, M. W.; Moss, D. S.; Thornton, J. M. In *PROCHECK*; Oxford Molecular: Oxford, UK, 1992; Vol. 2.